Crustal conductivity structure of a continental margin, from magnetotelluric investigations

Montahaie, M.[1*], Brasse, H.[2] and Oskooi, B.[3]

[1]*Ph D. Student of Geophysics, Earth Physics Department, Institute of Geophysics, University of Tehran, Iran*
[2]*Professor, Department of Earth Science, University of Berlin, Germany*
[3]*Assistant Professor, Earth Physics Department, Institute of Geophysics, University of Tehran, Iran*

Abstract

The deep internal structure of the crust can be determined using appropriate seismic and electromagnetic methods. The natural source magnetotelluric (MT) method is the most suitable electromagnetic technique for probing into the deep crust. A long period magnetotelluric data set obtained in the Southern Chilean Andes is investigated in this paper. Dimensionality analysis shows that the data may be regarded as with a strike 2D direction aligned to the N-S direction. Results of a joint inversion of different MT data types indicate relatively high conductive structures in the middle to deep crust beneath the volcanic arc.

key words: Magnetotelluric, Dimensionality analysis, Impedance, Inversion modeling

تعیین ساختار هدایت ویژه پوسته زمین در یک حاشیه قاره‌ای با استفاده از داده‌های مگنتوتلوریک

منصوره منتهایی ۱، هاینریش براسه ۲ و بهروز اسکوئی ۳

۱ دانشجوی دکتری ژئوفیزیک، گروه فیزیک زمین، مؤسسۀ ژئوفیزیک، دانشگاه تهران، ایران
۲ استاد، دانشکده علوم زمین، دانشگاه برلین، آلمان
۳ استادیار، گروه فیزیک زمین، مؤسسۀ ژئوفیزیک، دانشگاه تهران، ایران

چکیده

ساختار عمیق داخلی پوسته زمین با استفاده از روش‌های مناسب لرزه‌ای و الکترومغناطیسی مورد بررسی قرار می‌گیرد. ازمیان روش‌های الکترومغناطیسی روش مگنتوتلوریک که از منبع طبیعی (نوسانات میدان مغناطیسی زمین) استفاده می‌کند مناسب‌ترین روش برای کاوش پوسته پایینی زمین است. عمق کاوش در این روش بسته به بسامد نوسان‌های مورد استفاده تغییر می‌کند و هر چه بسامد کمتر باشد، ساختارهای عمیق‌تر بررسی می‌شوند. در این مقاله داده‌های مگنتوتلوریک بلند دوره (بسامد کوتاه) که در منطقه حاشیه قاره‌ای شیلی در امتداد دو نیم‌رخ شرقی-غربی و در عرض‌های جغرافیائی ۳۹٫۳ و ۳۸٫۹ درجه جنوبی برداشت شده‌اند، مورد بررسی قرار گرفته است. قطعه‌های زمین‌شناسی مهم که این دو نیم‌رخ از آنها می‌گذرند عبارت‌اند از: رشته کوه‌های موازی ساحلی (Coastal Cordillera)، دره طولی(Longitudinal Valley) و کمان آتشفشانی که دقیقاً زیر آتشفشان‌های فعال ویلاریکا (Villarrica) و لایما (Llaima) واقع شده است (شکل۱). مجموعاً ۳۲ ایستگاه در امتداد این نیم‌رخ‌ها با فاصله تقریبی ۱۰ کیلومتر از هم واقع شده‌اند و داده‌های مگنتوتلوریک را در محدوده دوره‌ای ۲۰٫۰۰۰−۱۰ ثانیه ثبت کرده‌اند.

مهم‌ترین مشکلی که در استفاده از این داده‌های MT دورۀ بلند وجود دارد، اثر واپیچش گالوانیکی ناشی از ناهمگنی‌های سه‌بُعدی کوچک محلی است که در قسمت‌های سطحی‌تر قرارگرفته و باعث می‌شوند که پاسخ‌های ناشی از ساختار عمیق دوبُعدی

---

*Corresponding author: Tel: 021-61118354   Fax: 021-88009560   E-mail: mmontaha@ut.ac.ir

منطقه‌ای پنهان شود. میزان انحراف داده‌های مگنتوتلوریک از مدل دوبُعدی منطقه‌ای با پارامتر پیچش (skew) اندازه‌گیری می‌شود. این مرحله که از آن تحت عنوان "تحلیل ابعادی" داده‌ها (dimensionality analysis) یاد می‌شود به روش بار (بار، ۱۹۸۸) صورت گرفته است. مقدار آستانه پارامتر پیچش در این روش برای تمایز بین ساختارهای ویژه هدایت دوبُعدی و سه‌بُعدی ۰٫۳ است. شکل۳ نمایش پربندی مقادیر پیچش محاسبه شده برای این دو نیم‌رخ است. این شکل نشان می‌دهد که مقادیر پیچش این داده‌ها به‌طورکلی بین ۰٫۳ و ۰٫۱ توزیع شده‌اند. بنابراین رویکرد دوبُعدی در مورد این مجموعه داده‌ها موجه است.

به‌منظور تفسیر داده‌های مگنتوتلوریک با استفاده از مدل‌های دوبُعدی ضروری است که یک جهت استرایک ثابت برای کل نیم‌رخ تعیین شود. تفسیر دوبُعدی داده‌ها فقط پس از چرخش آنها در جهت این استرایک امکان‌پذیر خواهد بود. در مورد این مجموعه از داده‌ها استرایک ساختار ویژه هدایت منطقه‌ای با استفاده از روش "تانسور فاز" برای هردو نیم‌رخ در جهت شمالی– جنوبی محاسبه شده است (شکل۴).

مدل‌سازی معکوس با استفاده از الگوریتم "گرادیان‌های مزدوج غیرخطی" و با استفاده از کد رودی و مکی (Rodi and Mackie, 2001) صورت گرفته است. فضای مدل با ۹۲ سطر و ۱۴۸ ستون مجزا شده و مدل اولیه از یک نیم‌فضای همگن با مقاومت‌ویژه ۱۰۰ اهم‌متر و اقیانوس با مقاومت‌ویژه ۰٫۳۳ اهم‌متر که محدوده آن با توجه به داده‌های عمق‌سنجی مشخص و تثبیت شده، تشکیل شده است. نتایج حاصل از مدل‌سازی معکوس داده‌های مربوط به این دو نیم‌رخ (شکل‌های ۵ و۶) بسیار شبیه به هم هستند و ساختارهای رسانای متمایزی را در پوسته میانی و پایینی نشان می‌دهند. این توده‌های رسانا به منزله سیالات موجود در نواحی گسلی منطقه و یا نواحی با گداختگی جزئی (واقع در کمان آتشفشانی) تفسیر می‌شوند.

واژه‌های کلیدی: مگنتوتلوریک، تحلیل بُعدپذیری، امپدانس، مدل‌سازی وارون

1 INTRODUCTION

Transfer functions which are estimated from magnetotelluric measurements consist of "impedance tensor" and "tipper vector". Impedance tensor elements relate the horizontal electric field with the corresponding horizontal magnetic field at the earth surface:

$$\begin{pmatrix} E_x \\ E_y \end{pmatrix} = \begin{pmatrix} Z_{xx} & Z_{xy} \\ Z_{yx} & Z_{yy} \end{pmatrix} \begin{pmatrix} H_x \\ H_y \end{pmatrix} \qquad (1)$$

Tipper vector $\vec{W} = \begin{pmatrix} W_x & W_y \end{pmatrix}^t$ is a complex transfer function between the vertical and horizontal geomagnetic field and is implemented as: (Schmucker, 1970)

$$\vec{B}_z(T) = W_x(T)\vec{B}_x(T) + W_y(T)\vec{B}_y(T) \qquad (2)$$

Where x, y, z denote Cartesian geomagnetic coordinates, $\vec{B}$ is magnetic induction and T is period. This complex vector is displayed as "induction arrows" for both real and imaginary parts:

$$\vec{P}(T) = \text{Re}\{W_x(T)\}\hat{i} + \text{Re}\{W_y(T)\}\hat{j}$$
$$\vec{Q}(T) = \text{Im}\{W_x(T)\}\hat{i} + \text{Im}\{W_y(T)\}\hat{j}$$
$$(3)$$

In a general 3D earth where $\rho = \rho(x,y,z)$ the form of $\underline{\underline{Z}}$ would be fully occupied. However assuming a 2D resistivity distribution beneath the earth where x and y are along and perpendicular to the strike direction, $\underline{\underline{Z}}$ would have an off-diagonal form with $|Z_{xy}| \neq |Z_{yx}|$ (Simpson and Bahr, 2005). This results from the fact that the derivatives of the fields vanish along the strike direction (x axis) and the fields decouple into the xy and yx modes, resulting in separated Maxwell's equations into two independent sets of differential equations, TE (transverse electric)and TM (transverse magnetic) polarization. In this case when plotting the real induction arrows on a map, they would point away from regions with high conductivities (Wiese, 1962). Because of these simplicities it is more popular to assume a regional 2D resistivity distribution

beneath the earth and then remove the effect of local shallower 3D heterogeneities that would distort the regional 2D structure responses.

In this study, the electrical resistivity structure at a continental margin formed by the subduction of the oceanic Nazca plate beneath the south American continent, between 38.5º S-39.5º S latitudes and

70º W-74º W longitudes, is investigated. Long period (T= 10-20000 s) magnetotelluric data from 32 stations have been considered.

Figure 1 displays the study area. MT stations in red triangles are along two E-W profiles at the latitudes 38.9˚s and 39.3˚s, extended from the Pacific coast to the

Chilean-Argentinean boarder. The main geological segments crossed by these profiles are: the Coastal Cordillera (CC), the Longtudinal Valley (LV) and the Volcanic Arc (VA) directly below active Llaima and Villarrica volcanoes.A NW-SE oriented fault system encompasses the arc and forearc between the trench and the Liquine-Ofqui mega shear zone. Fault traces are depicted by solid black lines in figure 1.

This study goes beyond an early work (Brasse and Soyer, 2001) by including tipper data in addition to TE and TM mode impedance data and a priori information like bathymetry data (Scherwath et al., 2006) and a highly resistive slab in the starting model.
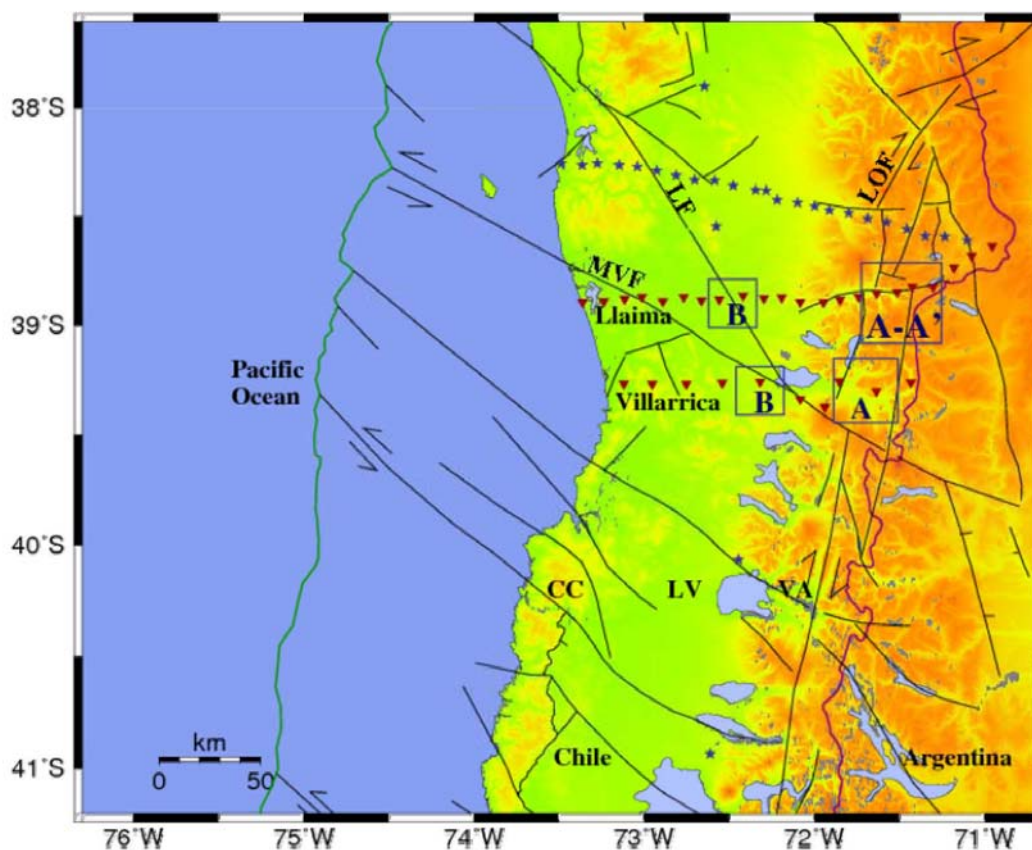

Figure 1. Map of the investigation area in the southern Andes. Stations in red color along Llaima and Villarrica profiles at latitudes 38.9˚ and 39.3˚ respectively are included in this study. Main geological segments: CC denotes Coastal Cordillera, LV Longtudinal Valley, VA Volcanic Arc. Major fault zones (black lines) referenced in the text are: LOF Liquine-Ofqui, LF Lanalhue, MVF Mocha-Villarrica. Dark-blue squares show the locations of resolved conductivity anomalies along Villarrica and Llima profiles.

2   MT DATA; DIMENSIONALITY AND REGIONAL STRIKES

The two profiles extend perpendicular to the coast line (the main structural boundary) from the Pacific coast to the Argentinean border and cross the Coastal Cordillera, Longitudinal Valley and the Volcanic Arc. They contain altogether 32 stations with a separation of about 10 km.

A crude image of electrical conductivity distribution can be obtained by the analysis of geomagnetic and electromagnetic transfer functions (tipper and impedance data, respectively).

Figure 2 displays typical features of MT responses (resistivity, phase and the real part of induction arrows) measured at sites representative of different geological segments. Response curves in figure 2 reveal that:

a) At the coastal sites the predominant effect (known as the "coast effect") is the large splitting of apparent resistivities and phases for xy and yx components (figures 2a and 2b), arising due to the high conductivity contrast between the ocean and the continent. However the induction vectors do not point W-E as it is expected for such a N-S directed conductivity contrast (in the presence of a simple 2D anomaly the real part of the induction vector would point away from the conductive structure and perpendicular to its strike (Wiese, 1962). Just at short periods, being dominated by the local bathymetry they are roughly W-E directed and at the longer periods the effect of an additional conductive anomaly in the dipper part is more significant (figure 2c).

b) Farther to the east, the coast effect becomes smaller in the Longitudinal Valley station data, both with regard to reduced splitting of xy and yx mode components (figures 2d and 2e) and the direction of the induction vectors, (they are not perpendicular to the shore line at short periods any more) and the resistivity values are smaller.

c) For the volcanic arc, higher resistivities are observed and the different mode splitting is more significant (figures 2g and 2h). Induction arrows at short periods indicate conductive anomaly at shallower depths in addition to the deep conductive body (figure 2i).

d) The induction vectors at station "cvo" display an outstanding behavior, they have large values even at short periods (T<15s) and point away to the north (figure 2l). This is the closest site to Villarrica volcano, where there is a lava lake in the crater at the top of the volcano. Thus a large scale magma deposit in the crust beneath the Villarrica volcano could be assumed.

e) Consistent feature in the geomagnetic transfer function of all different sites regardless of geological segments is the uniform deflection of induction arrows at long periods (figures 2c, 2f, 2i and 2l). This outstanding behavior could be regarded as a signature of anisotropy in this region (Brasse et al., 2008).

In order to interpret magnetotelluric data with the isotropic 2D inversion modeling, it is essential to determine a consistent regional strike direction for the whole profile. 2D interpretation of the data would be allowed when they have been rotated to the strike direction.

The departure of the impedance data from two dimensionality has been measured by calculating the skew parameters. This procedure which is called dimensionality analysis has been performed by the use of Bahr's (1988) approach in which it is assumed that near surface inhomogeneities distort the responses of the regional 2D conductive structure. In this approach the tentative threshold of the skewness value (phase sensitive skewness) to distinguish between 2D and 3D structures is 0.3 and higher values indicate 3D effects.
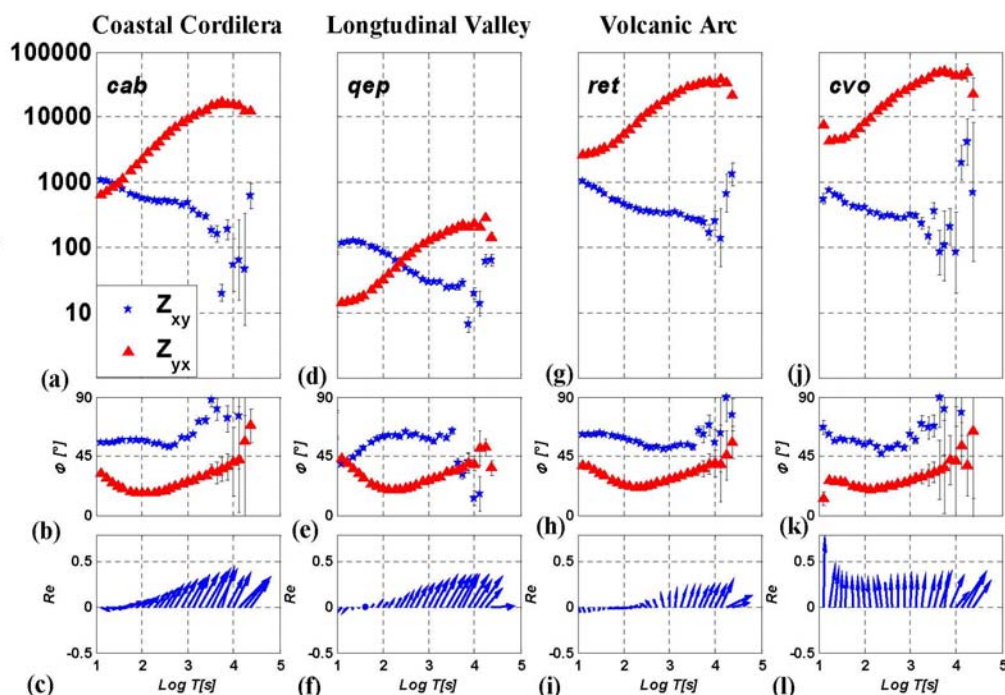
Figure 2. Transfer functions (apparent resistivities, phases and real part of induction arrows) in unrotated geomagnetic coordinates for representative stations in the Coastal Cordillera, Longitudinal Valley and Volcanic Arc. Red triangles show the transverse magnetic (TM) mode data and the blue stars show the transverse electric (TE) data. Data quality can be considered as good with the exception of period T>10000s for all sites. Spatial uniform deflection of induction arrows at long periods is remarkable (c, f, i, l). For further description see the text.

Figure 3 shows dimensionality analysis results of these two profiles as contour plots of calculated phase sensitive skewness (Bahr, 1988). It reveals that the whole data set may be regarded as 2D: in general, phase skew values are distributed between 0.1 and 0.3; just a few certain sites in the longitudinal valley have higher values. Accordingly a 2D approach is justified.

Regional strikes are calculated following the "phase tensor" scheme (Caldwell et al., 2004). In this approach the phase relationship contained in MT impedance data is considered as a second rank tensor," phase tensor". Decomposing the tensor to its SVD form, the orientation of the strike angle is determined as the direction which produces maximum or minimum impedance phases. Since there is no knowledge as to which of the maximum or minimum phases correspond to the TE or TM polarization, a 90º ambiguity remains in determining the strike

direction. In practice this ambiguity is resolved by the use of the vertical magnetic field data and consideration of regional geological strikes.

Figure 4 displays electric strike direction in rose diagrams for the two profiles and at different period bands (short, intermediate and long). It yields an average strike direction of 0º for the two profiles and just figure 4a shows a slightly greater scatter at short periods for the Llaima profile, due to the near surface anomalies which have greater influence at short periods. Accordingly the N-S direction (coincident with the main structural boundary) would be identified as the major strike direction for the whole profile. Since in MT method, fields are usually measured in geomagnetic coordinate system and in this region the average magnetic declination is approximately N 9º E this strike is almost perpendicular to the profile direction.
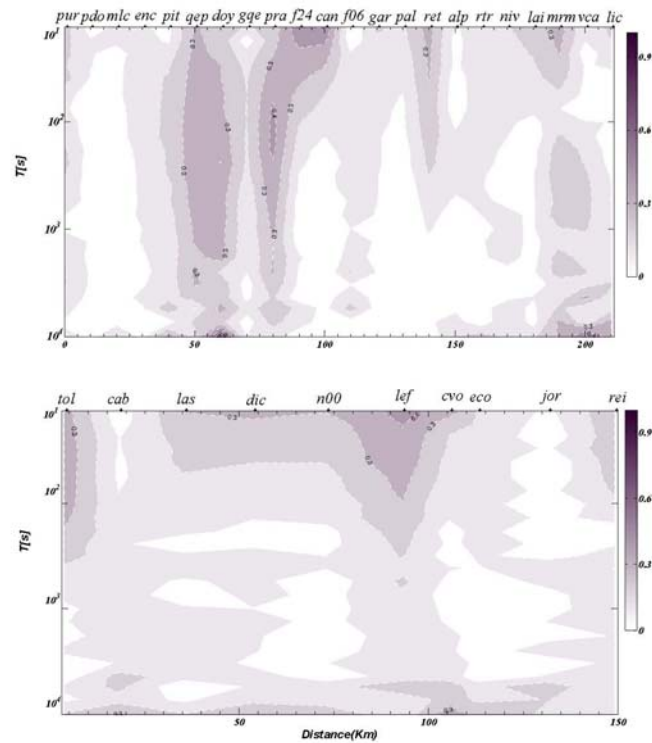
Figure 3. Contour plots of the impedance tensor Skewness in the Bahr definition for Llaima and Villarrica profile. Tentative measure for two dimensionality (skewness less than 0.3) is implemented by white and light colors. Accordingly a 2D approach for the data set could be justified.
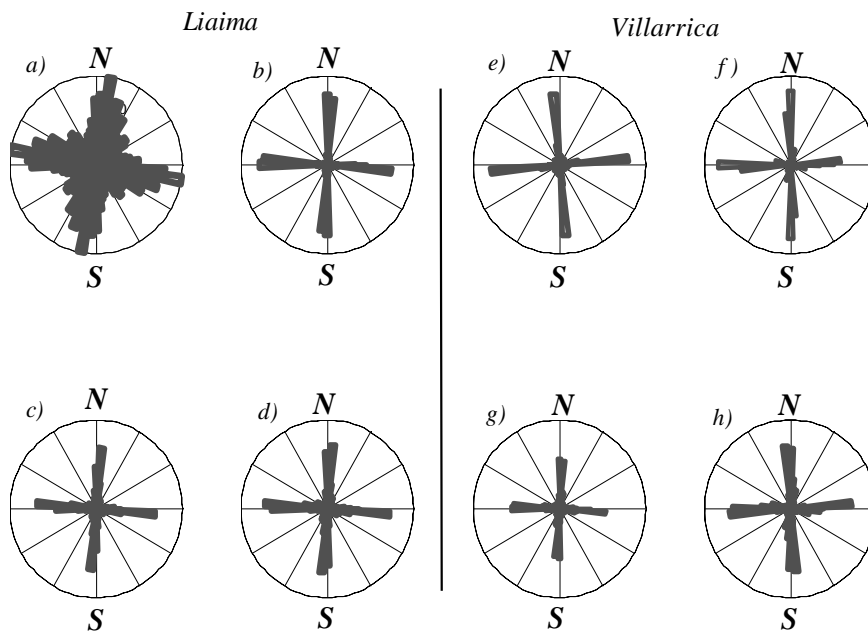

Figure 4. Rose diagrams showing electrical strike direction for Llaima (a-d) and Villarrica (e-h) profiles. Calculations made for different period bands: (a, e) 10-100 s, (b, f) 100-1000 s, (c, g) 1000-10000 s and the whole period range (d, h). It yields an averaged strike of N-S, almost perpendicular to the profile direction.

3 STANDARD ISOTROPIC 2D MODELING AND INTERPRETATION

Since the N-S direction is assumed as the major strike axis there is no need for rotating the data into the strike direction. 2D inversion modeling has been done by the nonlinear conjugate gradient

algorithm of Rodi and Mackie (2001). Models consist of 92 rows and 148 columns. A homogenous half space with 100 Ωm resistivity is used as the starting model. Due to its significant effect, the ocean with a crude bathymetry has been included and fixed as a priori information in the start model with a resistivity of 0.33 Ωm. Moreover a highly resistive slab of 1000 Ωm from the subducting Nazca plate has been incorporated in the start model. Its thickness and geometry are in accordance with the results of previous geophysical surveys in this region (Krawczyk et al., 2006). Individual error floors for TE and TM mode impedance data were relative errors of 20% for apparent resistivities and 5% (about 1.45 degrees) for phase data. Such a setting of error floors caused a higher weighting of phase data relative to resistivity in the inversion process thus reducing the influence of static shift effects, so the resulting model would have resistivity curves shifted with respect to the data while it could fit the phase data well. The static shift effect is further treated in the inversion code by calculating static shift factors so that the logarithm of these values would sum to zero. The minimum error floor for real and imaginary parts of tipper was set to 0.02. The regularization parameter which is selected as the value lying in the corner of the tradeoff curve (between data misfit and model roughness term in the objective function, usually an L-shape, (Asters et al., 2005) was set to τ=10.

Figures 5a and 6a display the final resistivity models obtained by jointly inverting tippers, TE and TM mode apparent resistivities and phases. Resultant data fit according to the root mean square error (RMS) for the final models are 1.4 for Villarrica and 1.9 for Llaima profile.

Figures 5a and 6a generally show similar significant structures:

The whole crust and even upper mantle has a relatively low resistivity of about 100Ωm except a resistive zone under the volcanic arc (structure E), more evident on the southern profile (figure 6a). Through the inversion process the resistive slab has been changed and become more heterogeneous.

Structure A-A': is the most significant conductor which exists in all different models It lies under the volcanic arc and its location has remarkable correlation with the intersection of the profile and the Liquine-Ofqui fault (LOF) zone (dark-blue squares in figure 1). Saline fluids in a fault system could be an explanation for the enhanced conductivity in this region. However there is an active volcano (Llaima volcano) in the north of the Llaim a profile near the station "ret" and thus the model may simply recover a large magma deposit.

Structure B: is another conductor in the west of the Central Valley section. It is located beneath the traces of Lanalhue and Mocha-Villarrica Faults so its high conductivity could originate from the saline fluids in the fault system. The other potential candidate, namely partial melts, is ruled out due to the low temperature in the forearc.

Structure A": The other highly conductive structure which is located in the easternmost of the profile and its geometry could not be resolved due to the lack of information outside the profile and only an extension of the profile could explain its origin.

Furthermore a small conductive feature (structure C) near the surface between the stations lef and cvo on the Villarrica profile (figure 6a) is resolved which could be supported by the sediments of Lago Villarrica lake just 2 kilometers in the north of the profile or it could be a signature of active volcanism owing to Villarrica volcano (station "cvo" is located at the foot of Villarrica volcano). The signature of this conductor on the northern profile is more evident when TE and TM mode data are jointly inverted (figure 5b between the stations "gar" and "f06").

A good conductor overlies the downgoing slab under the ocean (structure D, figure 5a). Although its origin remains mysterious its location is in good correlation with a strong seismic reflector under the northern most profile in figure 1 (Gross et al., 2008).
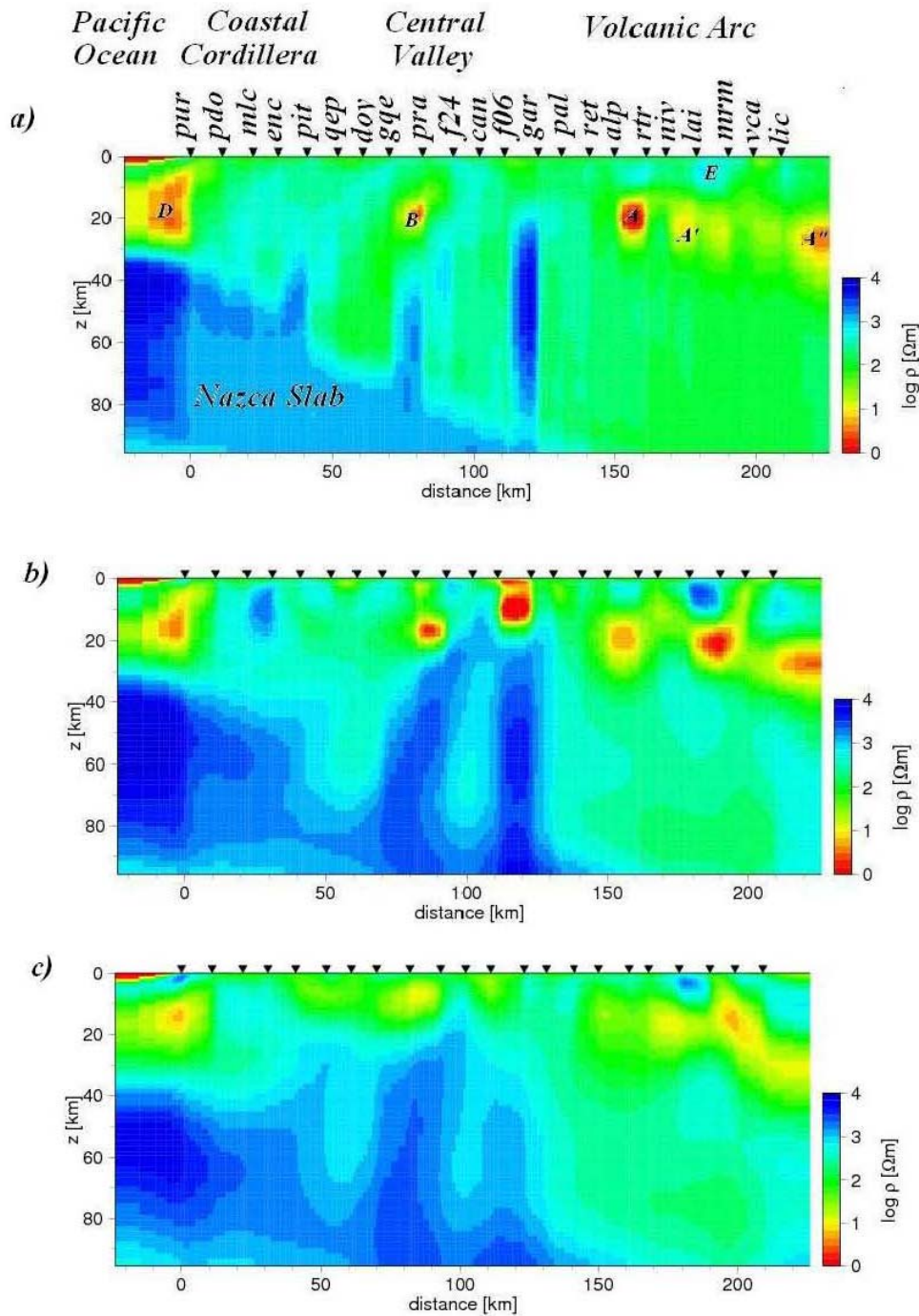

Figure 5. Inversion results for MT data along Llaima profile. a) Model is derived from jointly inverting TM, TE, and TP data, with an RMS of 1.9. b) Model is derived from jointly inverting TE and TM resistivity and phase data and converged to an RMS of 1.5. c) Model from inversion of only TM data with an RMS of 0.9. The warm colors represent regions of high conductivity and the colder colors represent resistive regions. The features A–E represent different structures consistent in each of the models. For further explanation about the resolved structures, see the text.
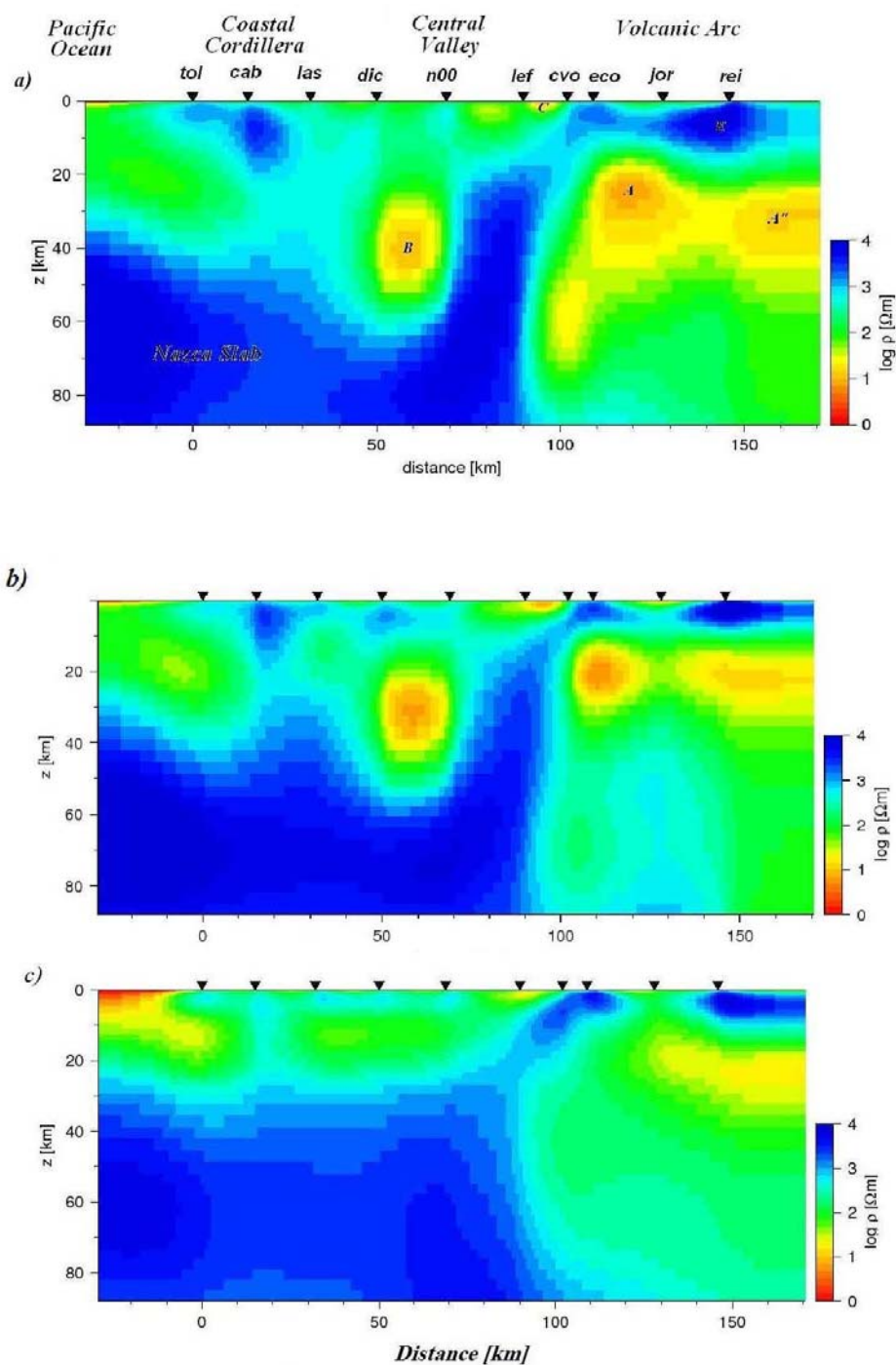
Figure 6. Inversion results for MT data along the Villarrica profile. a) Model is derived from jointly inverting TM, TE, and TP data, with an RMS of 1.4. b) Model is derived from jointly inverting TE and TM resistivity and phase data and converged to an RMS of 1.3. c) Model from inversion of only TM data with an RMS of 0.95. The warm colors represent regions of high conductivity and the colder colors represent resistive regions. The features A–E represent different structures consistent in each of the models. For further explanation about the resolved structures, see the text.
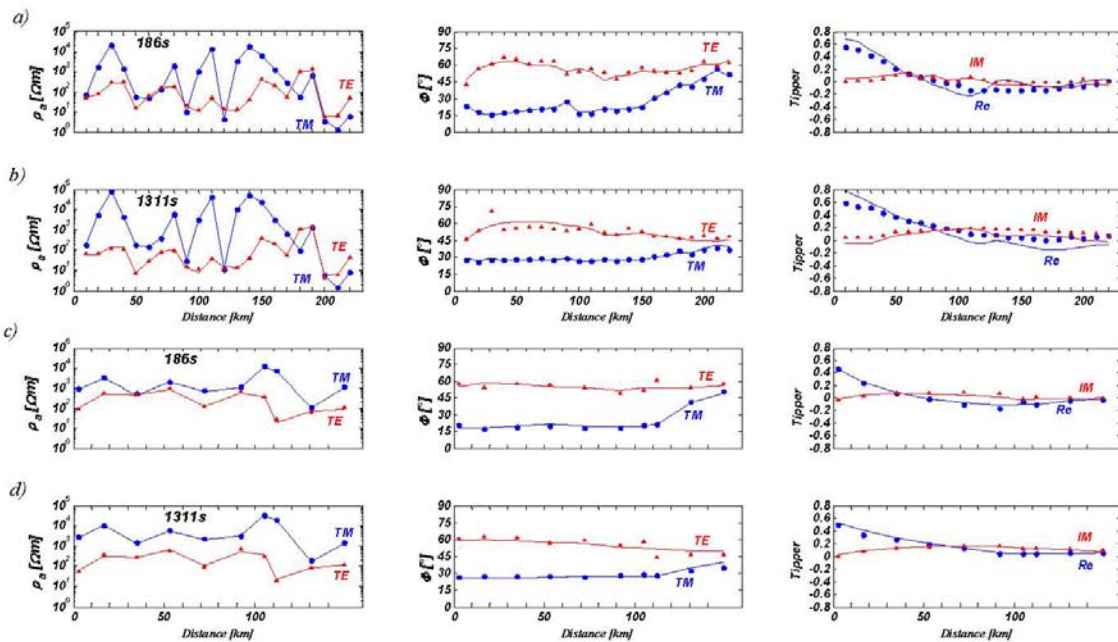
Figure 7. Characteristic fit of model response (solid lines) to data for different transfer functions (TE and TM apparent resistivity and phase, and real and imaginary part of tipper) at 186 and 1311s periods along Llaima (a-b) and Villarrica (c-d) profiles. Data fit could be considered generally good.

Many tests were conducted to find a reliable final model. The most important ones are considered in the following:

1) Since different magnetotelluric transfer functions (TE and TM mode impedance data and tipper) have different boundary conditions at conductivity interfaces their sensitivity to subsurface structures would be different (Wannamaker, 1999). Individual inversions with TM mode and TP data achieve RMS values of 0.95 and 1.6, respectively, while TE mode data results in an RMS about 3.4. Assigning a higher error floor (50%) to the resistivity TE mode data, the RMS would be 1.79 and in both cases the resulting models are similar and they recover a sharp and very strong anomaly under the volcanic arc. Inversion of TM mode data converges to a smooth model with the main conductor under the volcanic arc and the easternmost anomaly which is extended outside the profile (figure 5c).

So despite the shape and depth extent variation of the features between different models, conductors A-D, mentioned in figures 5a and 6a are consistently found.

2) The influence of different starting models was tested by assuming a homogeneous half space as a start model. Inversion results were quite similar to figures 5a and 6a.

3) Some experiments have been carried out to analyze the resolution of significant structures. Resistivities or geometrical borders of the significant structures were changed. Conducting a forward model, the resultant RMS would be checked then the inversion would start again to observe whether the significant conductors are resolved again and how their resistivities and locations have been modified. In this case study, replacing low resistivities with a more usual value of 50 Ωm the RMS increased to a higher value of 2.5 and conducting the inversion the conductor is resolved again after a few iterations.

Figure 7 illustrates the consistencies between measured and calculated TM, TE

and tipper responses. Data fit is generally good and exemplarily shown for periods of 186 and 1113s along the two profiles.

4 CONCLUSION

A long period MT data set along two profiles was investigated in this paper to obtain a crustal resistivity image of South Chile. Dimensionality analysis by the use of Bahr's (1988) method justifies a 2D approach of the data set and the regional strike based on the phase tensor method was calculated to be aligned to the N-S direction. Inversion results of Villarrica and Llaima profiles indicate distinct conductive features in the middle and deep crust. New inversion considerations used in this study (including tipper data and additional priori information incorporated in the start model) result in conductive features beneath both profiles which are more agreeable and their extensions are restricted better compared to the preliminary study of this data set .The conductive features are interpreted as fluids in the major fault zones (Liquine-Ofqui and Lanalhue faults) or partially molten regions beneath the volcanic arc.

Several inversions were conducted using different data subsets and start models to test the reliability of the obtained features for both profiles, whose most important ones are listed in section 3. All results were in general agreement with the final model. The resulting final model displays a plausible image particularly with respect to the resolved conductive bodies beneath the profiles whose locations have remarkable correlation with intersections of the profile and major fault zones (dark-blue squares in figure 1).

However, a more detailed investigation seems essential to explain SW-NE deflection of induction arrows especially at long periods. Additionally an extension of profiles to the east would provide explanation for the conductive feature in the east of both profiles.

REFERENCES

Asters, R. C., Borchers, B. and Thurber, C. H., 2005, Parameter Estimation and Inverse Problems: Int. Geophys. Ser., **90**, Elsevier, Amsterdam.

Bahr, K., 1988, Interpretation of the magnetotelluric impedance tensor: Regional induction and local telluric distortion: J. Geophys., **62**, 119–127.

Brasse, H. and W. Soyer, 2001, A magnetotelluric study in the southern Chilean Andes: Geophys. Res. Lett., 28, 3757–3760.

Brasse, H., Kapinos, G., Li, Y., Mütschard, L., Soyer, W. and Eydam, D., 2008, Structural electrical anisotropy in the crust at the South-Central Chilean continental margin as inferred from geomagnetic transfer functions: Phys. Earth Planet. In., 2008, doi:10.1016/j.pepi.2008.10.017

Caldwell, T. G., Bibby, H. M., and Brown, C., 2004., The magnetotelluric phase tensor: Geophys. J. Int., **158**, 457–469.

Gross, K., Miksch, U. and TIPTEQ Research Group, The reflection seismic survey of project TIPTEQ- the inventory of the Chilean subduction zone at 38.2°625 S, Geophys: J. Int., **172**, 565–571, doi:10.1111/j.1365-246X.2007.03680.x, 2008.

Krawczyk, C., Mechie, J., Lüth, S., Tašárová, Z. Wigger, P. Stiller, M., Brasse, H., Echtler, H. P., Araneda, M. and Bataille, K., 2006, Geophysical signatures and active tectonics at the South-Central Chilean margin, in The Andes - Active Subduction Orogeny: Frontiers in Earth Sciences, **1**, edited by O. Oncken et al., 171–192, Springer, Berlin, Heidelberg, New York.

Rodi, W. and Mackie, R. L., 2001, Nonlinear conjugate gradients algorithm for 2-D magnetotelluric inversions: Geophysics, **66**, 174– 187.

Schmucker, U., 1970, Anomalies of geomagnetic variations in the southwestern United States: Bull. Scripps Inst. Oceanogr., **13**, 165 pp.

Scherwath, M., Flueh, E., Grevemeyer, I., Tilmann, F., Contreras-Reyes, E. and Weinrebe, W., 2006, Investigating Subduction Zone Processes in Chile: EOS Trans: AGU, **87**, 265 pp.

Simpson, F. and Bahr, K., 2005: Practical Magnetotellurics, Cambridge Univ. Press.

Wannamaker, P. E., 1999, Affordable magnetotellurics: Interpretation in natural environments, in Three-Dimensional Electromagnetics: edited by M. Oristaglio and B. Spies: Soc. of Explor. Geophys., Tulsa, Okla. 349–374.

Wiese, H., 1962, Geomagnetische Tiefentellurik Teil II: Die Streichrichtung der Untergrundstrukturen des elektrischen Widerstandes, erschlossen aus geomagnetischen Variationen, Pure App. Geophys., **52**, 83–103.